PLANT SCIENCES

Mechanosensation in leaf veins

Tsu-Hao Yang, Aurore Chételat, Andrzej Kurenda†, Edward E. Farmer*

Whether the plant vasculature has the capacity to sense touch is unknown. We developed a quantitative assay to investigate touch-response electrical signals in the leaves and veins of *Arabidopsis thaliana*. Mechanostimulated electrical signaling in leaves displayed strong diel regulation. Signals of full amplitude could be generated by repeated stimulation at the same site after approximately 90 minutes. However, the signals showed intermediate amplitudes when repeatedly stimulated in shorter timeframes. Using intracellular electrodes, we detected touch-response membrane depolarizations in the phloem. On the basis of this, we mutated multiple *Arabidopsis* H^+*-ATPase* (*AHA*) genes expressed in companion cells. We found that *aha1 aha3* double mutants attenuated touch-responses, and this was coupled to growth rate reduction. Moreover, propagating membrane depolarizations could be triggered by mechanostimulating the exposed primary vasculature of wild-type plants but not of *aha1 aha3* mutants. Primary veins have autonomous mechanosensory properties which depend on P-type proton pumps.

INTRODUCTION

Plants can be exquisitely sensitive to gentle mechanostimulation. For example, touching stems can almost instantly block phloem carbon translocation in bean (*Vicia faba*) and in cotton (*Gossypium hirsutum*) (*1*). These findings highlight the fact that even gentle nondamaging touch stimuli have rapid effects on fundamental physiological processes underlying plant growth. Arguably better known than the rapid touch-response inhibition of carbon transport is the role of the phloem in electrical signaling in carnivorous plants. In many of these plants, prey capture is initiated when insects stimulate sensory hairs (trichomes) on the leaf epidermis. This is the case for the Venus flytrap (*Dionaea muscipula*) (*2*) and in sundews (*Drosera* spp.) (*3*). In the case of the Venus flytrap, electrical signals triggered by trap hair movements propagate in the phloem leading to trap closure, e.g., (*4*, *5*). Other touch responses appear to be largely trichome independent but still require electrical signaling in the phloem and possibly other vascular cell populations. This is, for example, the case of touch-stimulated leaf movements in the sensitive plant *Mimosa pudica* (*6*, *7*). Moreover, while the trichomes of *Arabidopsis thaliana* are clearly mechanosensory, e.g., (*8*, *9*), Arabidopsis leaves which lack trichomes still respond to gentle bending by producing the defense mediator jasmonate (*10*). This means that mechanosensory cell types might not be restricted to the epidermis. While electrical signals can be propagated in the phloem in response to leaf surface stimulation (*4*–*6*), the mechanosensory properties of sub-epidermal tissues or cell populations have not been studied in detail.

Using *A. thaliana* as a model, we focused on trichome-independent electrical events elicited by mechanostimulation of adult-phase leaves. A suitably rapid and reproducible assay was necessary for screening a large number of plants. Diverse methods have been used successfully to touch-stimulate Arabidopsis leaves. These include leaf bending (*10*, *11*), brushing (*9*, *12*–*14*), or falling water droplets (*9*, *15*). However, the forces (and durations) of stimulation applied with these techniques may differ between researchers. To investigate mechanosensation electrical signaling in the alga *Chara*, Shimmen (*16*) dropped glass tubing onto these giant cells. We developed a mechanostimulation method using spherical glass beads of known masses which were dropped onto leaf surfaces from a predetermined elevation. With video microscopy, we estimated dwell times on the leaf surface, and coupled to velocity calculations, we estimated applied forces. Using this simple method, we asked whether veins themselves respond to touch stimulation in the absence of extravascular tissues. That is, can veins act as mechanosensors and, if so, which cells in veins are likely to be mechanosensory? Previous work showed that the leaves of Arabidopsis produce electrical signals when they are brushed (*12*). However, whether this process is trichome dependent has, to our knowledge, not been reported. The Degli Agosti study (*12*) used electrodes inserted into leaf tissues. In the present work, we found that noninvasive surface electrodes also detected touch-response electrical signals in Arabidopsis. This allowed high-throughput analyses in which potential complications due to tissue damage could be eliminated. In this way, we were able to extend our study to genetic analyses with the goal of identifying genes involved in touch-response electrical signaling.

For mutational analyses aimed at altering mechanosensation-induced electrical signaling, we targetted *Arabidopsis* H^+*-ATPase* (*AHA*) genes expressed in the phloem. This gene family was chosen since it is largely responsible for maintaining plasma membrane potentials (*17*). Furthermore, AHA1 is known to help restore membrane potentials after wounding (*18*). The *AHA* family in *A. thaliana* has 11 representatives, and the experiments we performed took into account possible redundancy among members of this family as has been shown elsewhere, e.g., (*19*, *20*). Further complicating genetic analyses, loss-of-function mutations in some *AHA*s are male gamete-lethal (*21*). This precludes maintaining loss-of-function mutants and even generating homozygotes by crossing heterozygotes. We overcame this obstacle by using CRISPR-Cas9 mutagenesis and working with first-generation (T1) transformants carrying biallelic or homozygous mutations.

Department of Plant Molecular Biology, University of Lausanne, Lausanne, Switzerland.
*Corresponding author. Email: edward.farmer@unil.ch
†Present address: Vivent SA, Rue Mauverney 28, Gland 1196, Switzerland.

RESULTS

To develop a method suitable for the mechanostimulation of different parts of the leaf, we tested a protocol in which spherical borosilicate beads were dropped onto expanded leaves of 5-week-old rosettes. Noninvasive surface electrodes were placed at 0.5-cm intervals along the midvein acropetal to the bead impact site at positions E1′ and E2′ and basipetal to the impact site at positions E1 and E2 (Fig. 1A). Leaves were supported below the bead impact points and pickets, marked to indicate elevations for bead dropping (fig. S1), and were placed gently in the soil. Plants were then rested for 2 to 3 hours in the light. When 4-mm-diameter beads weighing 84.8 ± 1.0 mg were dropped 2 cm onto the adaxial petiole/lamina junction,

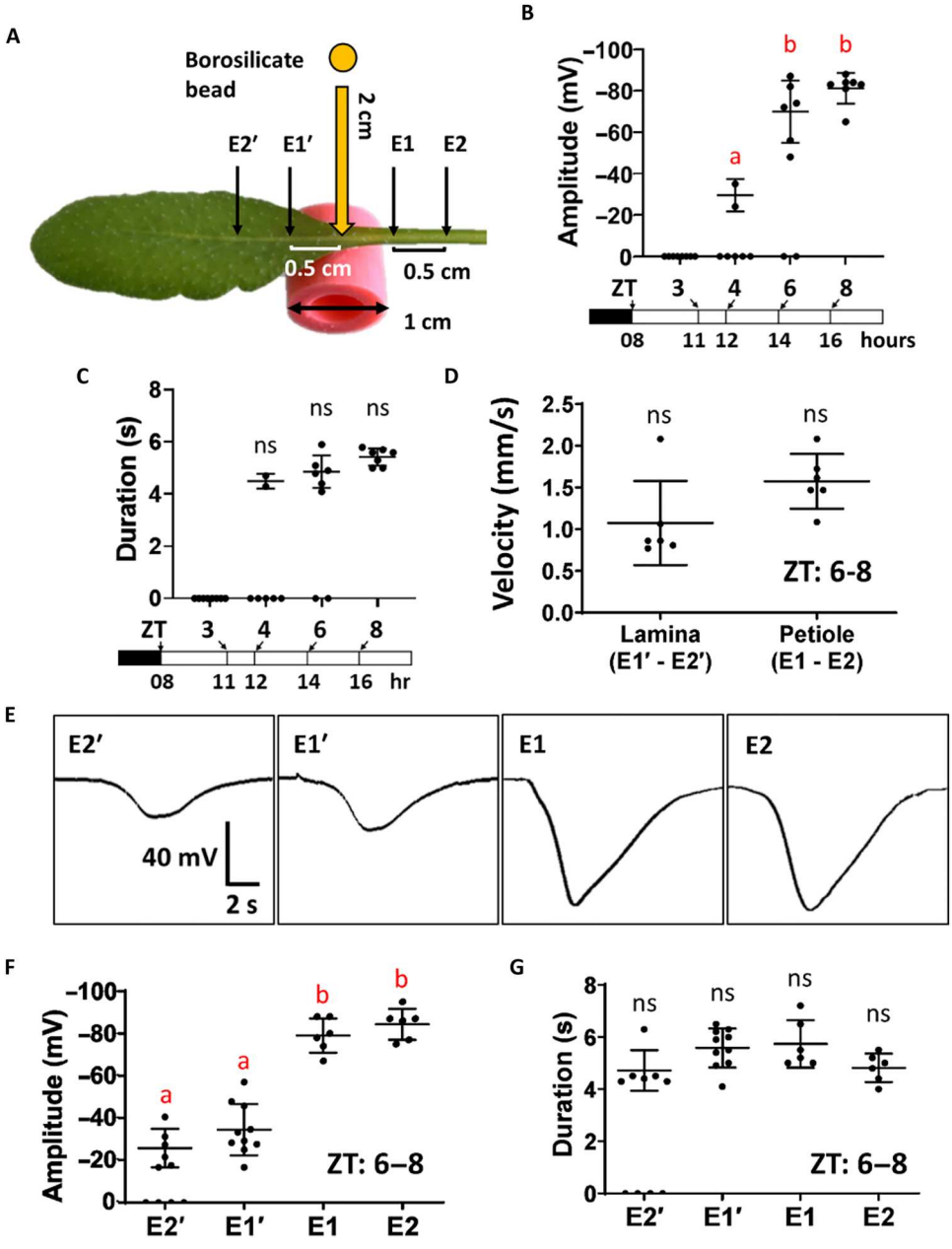

Fig. 1. Mechanostimulation-induced surface electrical signals in the WT. (**A**) Experimental design: Surface potential changes were recorded on the stimulated leaf in response to dropping an 84.8 ± 1.0 mg bead from an elevation of 2 cm onto the blade/petiole junction (yellow arrow). E1, E2, E1′, and E2′ represent the positions of surface electrodes. (**B**) Amplitude and (**C**) duration measured at electrode position E2 at 11:00, 12:00, 14:00, and 16:00 which represent the time points of 3, 4, 6, and 8 hours after ZT. Bars are means ± SD (n = 7 to 8). Letters indicate significant differences, Tukey post hoc test: $P < 0.05$. Data were from two combined experiments (one for 11:00/14:00 and one for 12:00/16:00). (**D**) Velocities of electrical signal between electrodes. Bars are means ± SD. (n = 6). Student t test: $P < 0.05$. ns, not significant. (**E**) Representative surface potentials at the different electrode positions. (**F**) Amplitudes for electrical signals detected at different electrode positions. (**G**) Duration for electrical signals detected at different electrode positions. Data points on the abscissa were not used for statistical analyses. Bars are means ± SD. (n = 6 to 10). Letters indicate significant differences, Tukey post hoc test: $P < 0.05$. Data in (D) to (G) are from experiments performed between 14:00 and 18:00 (ZT = 6 to 9). Data in (F) and (G) were from two combined experiments (one for E1′/E2′ and one for E1/E2).

this stimulated electrical signaling. However, during these initial experiments, we noted that electrical signals were detectable in afternoons but not in mornings. We therefore monitored the electrical responses of Arabidopsis rosettes to bead stimulation at different times of day. No electrical responses were detected at a Zeitgeber time (ZT) of 3 hours, and responses were intermediate at ZT = 4 hours (Fig. 1, B and C). At 6 hours after lights were switched on (ZT = 6), the responses monitored at electrode position E2 were similar to those monitored 8 hours (ZT = 8) after lights on (Fig. 1, B and C).

In the wild type (WT), the velocities of the electrical signals measured between electrodes either side of the impact site were similar (1.0 to 1.5 mm/s, equating to 6 to 9 cm/min) (Fig. 1D). Depending on electrode placement, the electrical signals had different architectures. In general, the signals were slightly asymmetrical with the depolarization phase being of shorter duration than the repolarization phase (Fig. 1E). Signals were detected at the E1′ and E2′ positions on the midvein were of significantly lower amplitude compared to those measured on the petiole and the electrode placed at the E2′ position failed to reproducibly detect events triggered by falling beads (Fig. 1F). That is, signal amplitudes were highest on the basipetal petiole and lowest nearer the leaf apex. Depolarization durations recorded on the petiole and on the midvein was similar and fell in the region of 4 to 6 s (Fig. 1G).

Repeated mechanostimulation generates signals with intermediate amplitudes

We calculated the theoretical momentum of a 4-mm-diameter bead released from 2-cm elevations (fig. S2A). Then, using video microscopy, we measured dwell times of the beads between the moment they contacted the adaxial midvein at the lamina/petiole junction until the moment they lost contact after rebounding (fig. S2B). On the basis of these recordings, an average force of 38 mN was calculated for the 4-mm-diameter beads weighing 84.8 ± 1.0 mg (fig. S2, C and D). From extrapolation of these data, we estimated forces for the following beads also dropped from 2-cm elevations onto lamina/petiole junctions: 2-mm diameter (7.1 ± 0.8 mg): 3.2 mN; 3-mm diameter (38.6 ± 1.9 mg): 17 mN; 5-mm diameter (169.7 ± 2.2 mg): 76 mN. In summary, dropping 4-mm-diameter beads 2 cm onto the leaf/petiole junctions reproducibly triggered electrical signaling that could be detected along the main vein on either side of the impact site. The three other bead diameters (2, 3, and 5 mm) were investigated for their abilities to trigger electrical signals recorded at electrode E2. These experiments shown in fig. S3 (A and B) revealed that 5-mm-diameter beads dropped 2 cm onto petiole/lamina junctions and exerting an estimated force of 76 mN triggered reproducible surface potentials monitored at the E2 (basipetal petiole) position. Three-millimeter-diameter beads exerting a calculated force of 17 mN also triggered reproducible signals. However, 2-mm-diameter beads (3-mN estimated force) did not consistently elicit electrical activity in the assay. In each case, when electrical signals were detected at the same position on the leaf, they had similar amplitudes and durations. We then asked whether these signals corresponded to action potentials (APs).

APs are all-or-none signals with discrete refractory periods (*22*). We investigated whether there was a refractory period between electrical signals triggered by bead mechanostimulation. To do this, beads were dropped twice onto the same site at the petiole/lamina junction, and electrical signals were monitored at electrode position E2. When 4-mm-diameter beads were dropped onto leaves with only 30- or 60-min intervals between stimulations, the second signals were of intermediate amplitudes. The resting time necessary to produce a second depolarization amplitude similar to the first one was in the order of 90 min (Fig. 2, A and B). We noted that similar timeframes were reported for the recovery mechanostimulation-inhibited phloem transport (*1*).

Electrical activities are trichome-independent and activate the jasmonate pathway

Arabidopsis trichomes are mechanosensory (*8*, *9*). The *Arabidopsis glabra1-1* (*gl1-1*) mutant lacks trichomes and has altered cuticular properties (*23*). Electrical activity was monitored at electrode position E2 in response to dropping 4-mm beads onto the lamina/petiole junction of *gl1-1*. Compared to the WT, we found no significant effect of *gl1-1* on electrical events with our assays (fig. S4A). To test whether mechanostimulation-induced surface potentials required a functional jasmonate pathway, we used the same assays this time with a loss-of-function *allene oxide synthase* (*aos*) mutant (*24*). This mutant did not affect surface potential production in our assays (fig. S4B). Mild mechanostimulation stimulates activity of the jasmonate pathway (*10*, *25*, *26*). To investigate induction of jasmonate signaling, a reporter gene comprising the jasmonate-inducible *ALLENE OXIDE SYNTHASE* (*AOS*) promoter driving expression of nuclear-localized Venus fluorescent protein *AOSpro::*3x-NLS-Venus (*27*) in the WT was used. Fluorescent imaging 4 hours after bead dropping showed reporter activation near the bead drop site (fig. S4C). We found that bead stimulation caused the accumulation of *AOS* transcripts in WT plants (fig. S4D).

Electrical signals are detected after mechanostimulating exposed veins

We next compared electrical responses measured over the midvein to those in the lamina. Using the experimental design shown in Fig. 3A, we found that dropping 4-mm-diameter beads onto petiole/lamina junctions elicited signals in the lamina (monitored at the E2″ position) that had different architectures (Fig. 3B), lower amplitudes, and shorter durations (Fig. 3C) than those detected on the primary vein at position E1′. We then tested whether touch-response electrical signals could propagate through vein tissue from which extravascular cells had been removed. Sections of the petiolar primary vein approximately 1 mm long were surgically exposed as shown in Fig. 3D. Electrical signals generated by mechanostimulation could be detected distal to the site of extravascular tissue removal (Fig. 3E).

To investigate the possibility that the vasculature could itself act as a mechanosensor in the absence of extravascular tissues, primary veins from expanded leaves were exposed as described previously (*28*). This method involves gently pulling the petiolar sheath off the main vein, leaving the exposed vein attached to the petiole as illustrated in Fig. 3F. For experiments, veins were exposed in the morning at ZT = 1 to 2 hours and were immediately laid on glucose-containing agar strips as shown in Fig. 3G. The plant was then placed in the light at high humidity for a further 4 hours. At that time, beads (4-mm diameter, 85-mg masses) were dropped from an elevation of 2 cm onto the vein at a distance of 1 cm from where it was attached to the petiole. Electrodes on the petioles were used to monitor mechanostimulated electrical activity. In four of nine experiments, electrical signals were successfully monitored

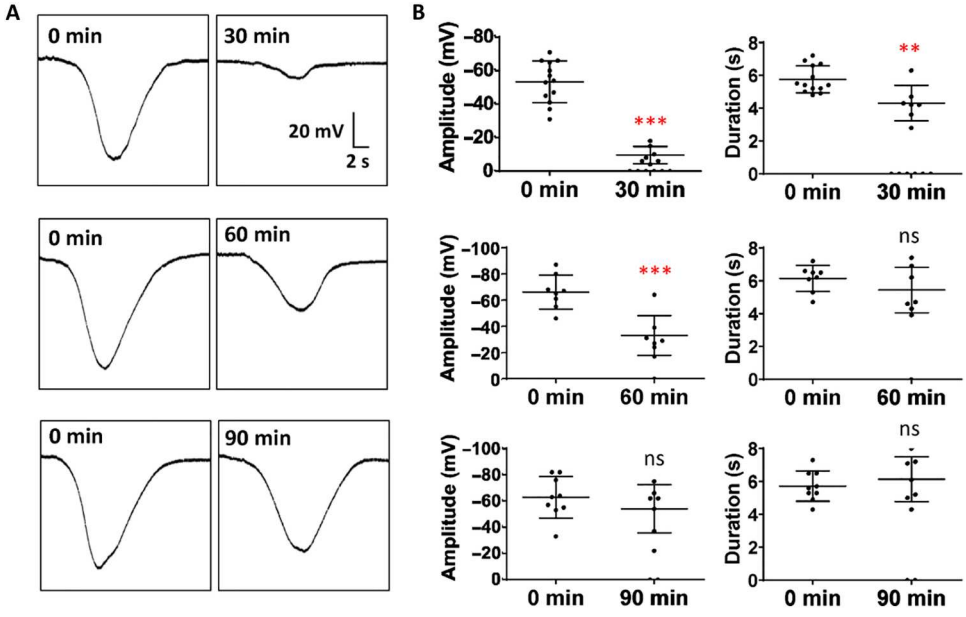

Fig. 2. Characteristics of mechanostimulation-induced surface electrical signals. The monitoring electrode was placed at position E2, and beads were dropped onto petiole/lamina junctions. The distance between E2 and the bead impact site was 1 cm as shown in main Fig. 1A. Experiments were performed between 14:00 and 18:00 (ZT = 6 and 9). (**A**) Representative surface potential changes of two consecutive bead (85 mg) stimulations on the same plant with 30-, 60-, and 90-min intervals. (**B**) Amplitude and duration. Data points on the abscissa were not used for statistical analyses. Bars are means ± SD. (n = 8 to 13). Student t test: ***P < 0.001, **P < 0.01. All the recordings were measured at electrode position E2.

in the intact petiole distal to the bead impact site on the vein (Fig. 3H). These signals had amplitudes (approximately 20 mV; Fig. 3H) lower than those measured at the same position in intact plants (Fig. 1F). To further examine vascular autonomy in mechanosensation, we used WT plants expressing the cytosolic Ca^{2+} reporter GCaMP3 under the *UBIQUITIN 10* promoter (*29*). When beads were dropped onto the exposed primary veins of these plants, Ca^{2+} signals propagated basipetally away from the impact site (movie S1).

Having established that veins could produce electrical signals, we investigated whether phloem cells were excitable in response to bead stimulation. Using the aphid *Brevicoryne brassicae* as a living electrode with which to probe plant-derived electrical activity (*30*), we probed sieve elements during mechanostimulation. Beads of diameter 5 mm were dropped from 2 cm above the leaf onto the lamina/petiole junction to apply mechanostimulation. Aphids fed most frequently on the laminal midvein (equivalent to position E1′) approximately 1 cm from the bead impact site (Fig. 4A). Induced membrane potential changes were monitored during the aphid feeding phase as described (*30*). A representative signal is shown in Fig. 4B. Additional measurements under the same conditions were used to monitor surface potentials. Phloem signals had similar amplitudes to surface potentials (Fig. 4C), but the durations of the phloem signals were significantly shorter than those of the surface potentials (Fig. 4D).

glr and *msl10* mutations affect mechanostimulated electrical activity

Ion channels with genetically verified roles in wound-response electrical signaling include GLUTAMATE RECEPTOR-LIKE (GLR) GLR3.3 and GLR3.6 (*31*) and MscS-Like 10 (MSL10) (*32*). Mutants in the genes encoding these proteins were tested in the mechanostimulation assay. The *glr3.3 glr3.6* double mutant attenuated membrane depolarization amplitudes (fig. S5A) but did not affect their durations (fig. S5B). By contrast, an *msl10* mutant did not display significantly altered membrane depolarization amplitudes (fig. S5C). Signal durations were diminished at bordlerline significance in *msl10* relative to the WT (fig. S5D). We then sought further genes which might function in touch-response electrical signaling.

Proton pumps underlie touch-response membrane potential changes

Using three guide RNAs per gene (table S1), we targeted a quartet of *AHA*s (*AHA1*, *AHA3*, *AHA8*, and *AHA11*) that are most abundantly expressed in phloem companion cells according to You *et al.* (*33*). These experiments produced two lines (A11 and A24) with clearly defined mutations in *AHA1* and *AHA11* (fig. S6, A and B). No mutations in *AHA3* or *AHA8* were detected in these plants, and the plants at the T1 stage all had WT-like growth rates and phenotypes (fig S6, C and D). Using the experimental design in fig. S6E, no effect of the *aha1 aha11* double mutant on mechanosensation was detected (fig. S6, F and G). From the same transformation, one line carrying a putative homozygous mutation(s) in *AHA3* and a putative heterozygous mutation(s) in *AHA8* (line 21) was backcrossed with the WT and genotyped (Fig. 4E) using primers shown in table S2A. Seeds from the backcross were selected, and plants carrying putative homozygous *aha3* mutations were tested in the bead assay (Fig. 4F). A weak but statistically significant reduction in membrane depolarization amplitude relative to the WT was detected in these plants (Fig. 4G). Pollen carrying loss-of-function *aha3* mutations is not viable (*21*), and we found that plants carrying putative homozygous or biallelic *aha3* mutations were sterile (Fig.

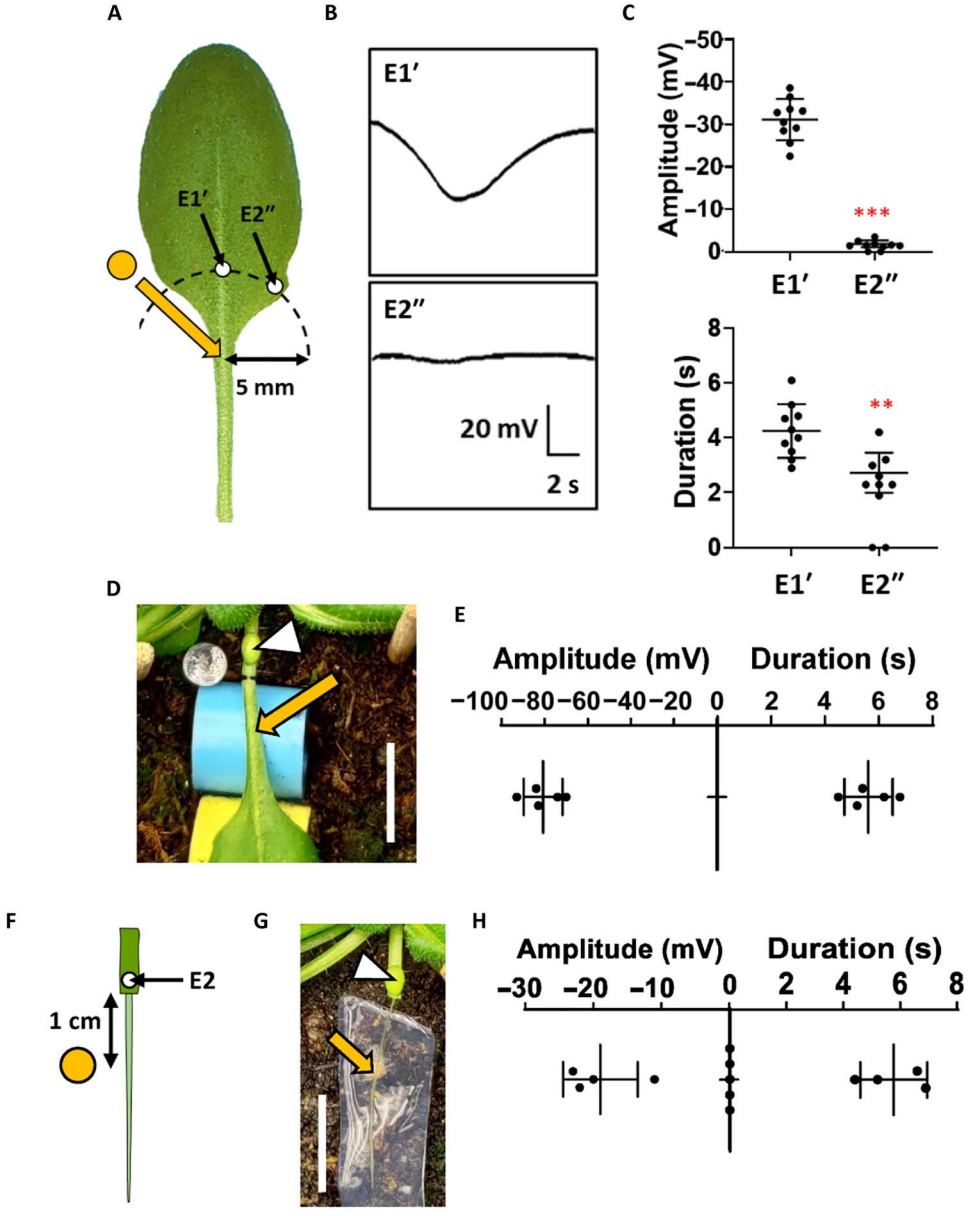

Fig. 3. Mechanosensation in the primary vein. (**A**) Experimental design: E1′ and E2″ are the positions of surface electrodes. Electrodes were 5 mm distant from the stimulation site indicated with a yellow arrow. The support below the stimulation site is not shown. (**B**) Representative surface potential changes recorded on the stimulated leaf in response to dropping an 85-mg bead from an elevation of 2 cm onto the blade/petiole junction. (**C**) Amplitude and duration (n = 10). (**D**) Experimental design to test signal propagation through a vein lacking surrounding tissues. Scale bar, 1 cm. (**E**) Amplitude and duration of signals transmitted through veins lacking surrounding tissues. (n = 5) (**F**) Scheme showing exposed vein and placement of the recording electrode (E2). The bead impact site is 1 cm from the petiole sheath. (**G**) Experimental design for vein mechanostimulation. Scale bar, 1 cm. For (D) and (G), electrode position (white arrowhead) and bead impact site (orange arrow). (**H**) Amplitude and duration (n = 9). Data points on the abscissa were not used for statistical analyses. Bars are means ± SD. Student t test: $^{**}P < 0.01$, $^{***}P < 0.001$. Experiments were performed between 14:00 and 18:00 (ZT = 6 to 9).

4H). Given the weak effect of *aha3* mutation and potential complexities from mutated *aha8*, these experiments were considered to be insufficient.

Work on *AHA8* was abandoned and we focused on obtaining *aha3* mutations in *aha1 aha11* backgrounds. For this, the A11 double mutant was retransformed with guide RNAs targeting *AHA3*. A portion of these T1 plants displayed clearly reduced growth rates (fig. S7A). The *AHA3* alleles in these plants were sequence-confirmed (table S3) using primers shown in table S2B. Eight verified *aha1 aha3 aha11* triple mutants were bead-stimulated (fig. S7B) and were found to have strongly altered membrane depolarization amplitudes relative to the WT (fig. S7C). These plants did not produce siliques (fig. S7D). These data indicated that loss of function in *AHA3* in the *aha1 aha11* background strongly affected mechanosensation. To discover which of the two mutated *AHA*s (*AHA1* or *AHA11*) enhanced the weak mechanosensation

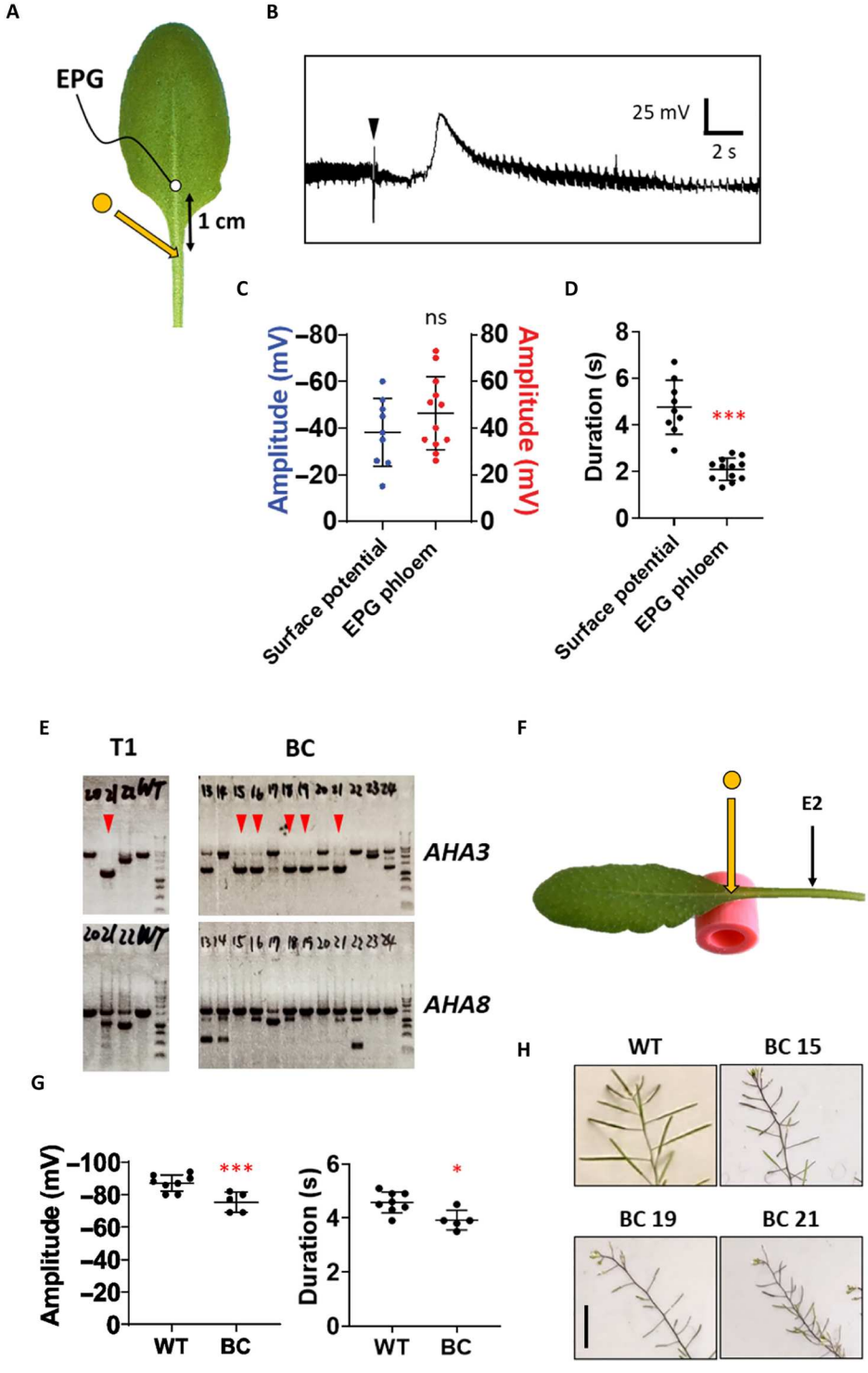

Fig. 4. Mutations in phloem-expressed *AHA*s attenuate mechanoresponse electrical signaling. Detection of touch-response electrical signals in phloem sieve elements. (**A**) Experimental design. The bead impact site is indicated with a yellow arrow. EPG represents the electrical penetration graph (EPG) electrode attached to a feeding aphid (white circle). (**B**) Recording of phloem electrical activity. The black arrowhead indicates the moment of stimulation; 5-mm-diameter bead dropped 2 cm onto the petiole of the leaf. Note that the leaf was not supported. Amplitude (**C**) and duration (**D**) of mechanostimulation-induced surface potentials measured in the same region and phloem electrical signals. Surface electrode: $n = 9$; phloem electrode: $n = 12$. Error bars are mean ± SD. Student t test: $^{***}P < 0.001$. Experiments were performed between 14:00 and 18:00 (ZT = 6 to 9). Biallelic *aha3* CRISPR-Cas9 mutations attenuate mechanostimulation-induced electrical signals. (**E**) Genotyping PCR for *AHA3* and *AHA8*. Red triangles indicated the biallelic *aha3* mutants in T1 (no. 21) and in backcrossed (BC) generations. (**F**) Experimental design. Four-millimeter diameter (85 mg) beads were used to stimulate leaves the blade/petiole junction (yellow arrow). Electrical signals were measured at the E2 position. (**G**) Amplitude and duration of mechanostimulation-induced electrical signals. Bars are means ± SD. ($n = 5$ to 8). Student t test: $^{***}P < 0.001$; $^{*}P < 0.05$. (**H**) Siliques of WT and male-sterile *aha3* mutants. Scale bar, 1 cm.

phenotype of loss-of-function *aha3* mutants (Fig. 4G), two double mutants were produced: *aha1-7 aha3* in which the *aha1-7* Transfer-DNA (T-DNA) insertion mutant from (*18*) was used and *aha3 aha11*. The *aha1-7 aha3* mutants grew more slowly than the WT (Fig. 5A) and were infertile (Fig. 5B). When tested in mechanostimulation assays (Fig. 5C), *aha1-7 aha3* showed a strong reduction in mechanosensation-induced electrical signal amplitude with a statistically insignificant effect on duration (Fig. 5D). Sequencing of the *aha1 aha3* and *aha3 aha11* lines tested confirmed that they carried homozygous or biallelic *aha3* mutations (table S3). The *aha3 aha11* mutants showed no evident mechanosensation phenotypes (fig. S8A); however, we noted weakly reduced growth rates (fig. S8B) and infertility (fig. S8C). Using the experimental design in Fig. 5E, we then compared the mechanosensitivity of WT and

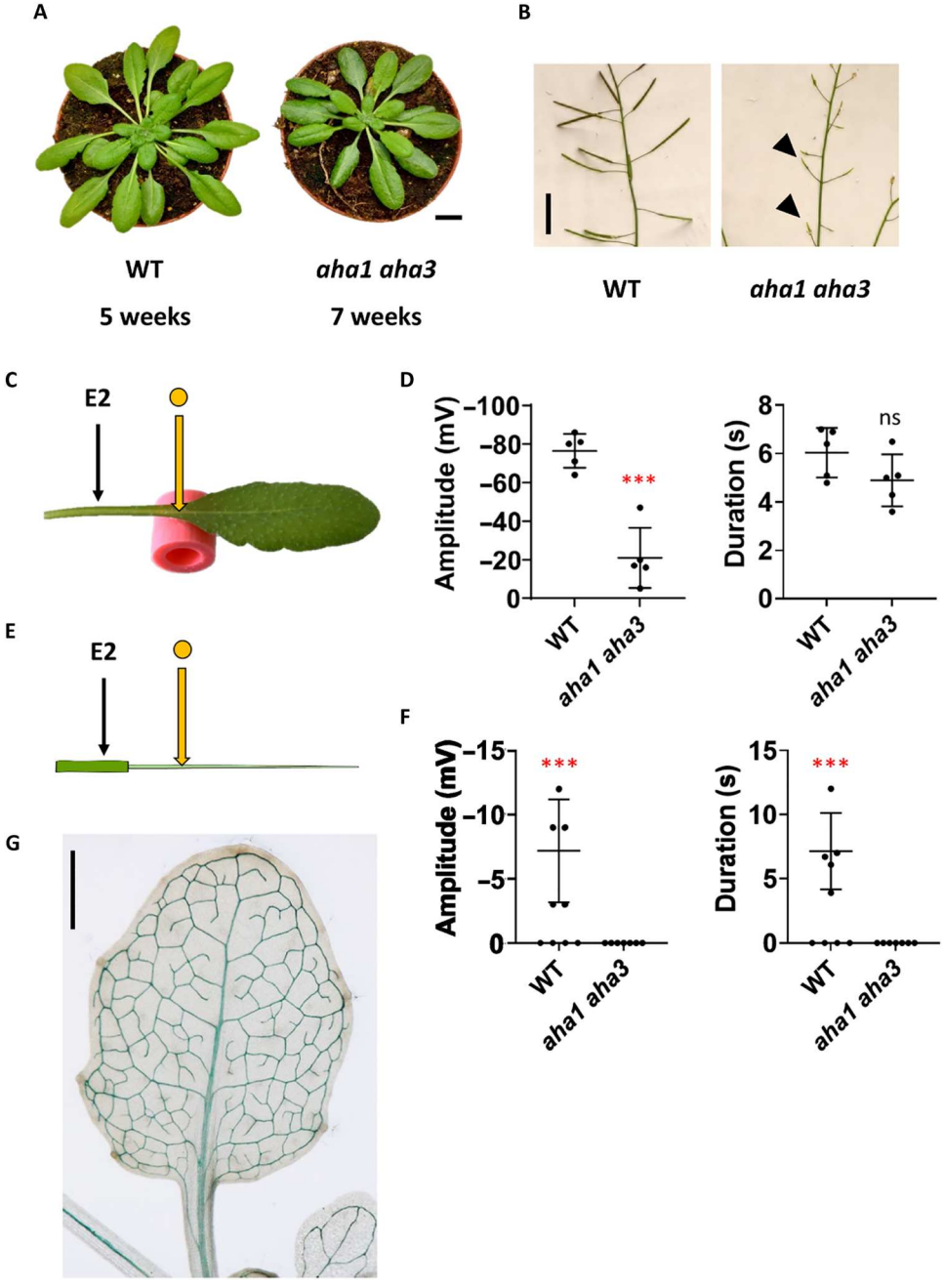

Fig. 5. Effect of *aha1 aha3* mutations on mechanostimulation-induced electrical signals. (**A**) Rosette phenotype of 5-week-old WT and 7-week-old *aha1 aha3* plants. Scale bar, 1 cm. (**B**) Siliques of WT and *aha1 aha3*. Arrowheads indicate failure of *aha1 aha3* to produce siliques. Scale bar, 1 cm. (**C**) Experimental design for mechanostimulation of leaves. Plants were stimulated by dropping a 4-mm-diameter bead from an elevation of 2 cm onto the blade/petiole junction (yellow arrow). (**D**) Amplitude and duration of mechanostimulation-induced electrical signals in leaves. Bars are means ± SD (n = 5). Student t test: ***P < 0.001. (**E**) Experimental design for mechanostimulation of exposed veins with 4-mm-diameter beads. The yellow arrow indicates the impact site. (**F**) Amplitude and duration of mechanostimulation-induced electrical signals in veins. Data points on the abscissa were not used for statistical analyses. Bars and means ± SD (n = 7 to 9). Student t test: ***P < 0.001. (**G**) Staining pattern produced by $AHA3_{pro}$::*AHA3-GUS* expression in a leaf of a 4-week-old plant. Scale bar, 1 mm. The *aha1-7* allele from (*18*) was used to construct *aha1 aha3* mutants.

aha1-7 aha3 veins. Approximately half (five of nine) of WT veins produced electrical signals in response to bead stimulation, whereas these signals were invariably undetectable in the mutant (Fig. 5F). Last, DeWitt and Sussman (*34*) discovered AHA3 protein in companion cells in major and minor leaf veins. Plants expressing an $AHA3_{pro}$::AHA3-GUS fusion protein were generated. β-Glucuronidase activity was observed in all three leaf vein orders throughout the leaf (Fig. 5G).

DISCUSSION

The touch-response signal is not an AP

Using parallel experimental designs and genetic analyses, we detected and manipulated touch-response electrical signals in both leaves and veins. Mechanostimulation-induced electrical signals in leaves were undetectable in the first 3 hours of morning light, becoming reproducibly detectable approximately 6 hours after illumination. The transcript levels of many touch-inducible genes in Arabidopsis increase in darkness (*11*). However, we are unaware of reports of time-of-day–dependent mechanosensitivity or electrical signaling in this plant. APs in metazoans are typically all-or-none signals. That is, after a refractory period, the signal produced by a second stimulus to the same individual is essentially identical in amplitude to that produced by the first stimulus (*22*). Signals with these characteristics are well known in plants, for example, the Venus flytrap, e.g., (*35*). By contrast, intermediate amplitudes were generated in Arabidopsis when the interval between successive bead mechanostimulations was less than 90 min. This distinguishes the signals we monitored from canonical APs. Other non-AP signals, typically with longer durations than those we measured, can be produced in response to stem bending (*36*).

P-type proton pumps function in mechanosensation

We found that a *glr3.3 glr3.6* double mutant in which leaf-to-leaf wound-response electrical signaling is impaired (*31*), also weakly attenuated touch-induced electrical signals. Finding an impact of this double mutant on touch-response electrical signaling highlights a partial mechanistic overlap between touch and wound signaling. However, since *glr3.3 glr3.6* failed to eliminate touch-response signals, we sought other genes which might play a role in this process. The diverse mechanisms of mechanosensation in bacteria (*37*), mammals (*38*), insects (*39*), and plants (*40*, *41*) all require transmembrane ion and/or proton fluxes, and several ion channels potentially involved in leaf mechanosensation have been identified (*42*, *43*). In contrast, the roles of proton pumps in mechanosensation are poorly characterized. AHAs are primary determinants of membrane potential in plants (*17*), and the touch-induced movements in *M. pudica* are thought to depend on proton pumps (*44*). This, and the fact that touch-stimulated electrical signals could be detected in sieve elements, led us to target four proton pumps expressed in the phloem: *AHA1*, *AHA3*, *AHA8*, and *AHA11*. Since the *AHA3* gene is essential for pollen viability (*21*), we had to work on T1 generation plants and to create homozygous or biallelic mutants in single rounds of CRISPR-Cas9 mutagenesis. Initial findings that *aha3* mutation weakly attenuated electrical signaling prompted further CRISPR-Cas9 mutagenesis, which led to the finding that strong electrical signal attenuation occurred in *aha1 aha3* double mutants.

What, if any, is the biological relevance of the observations of diel electrical signaling in response to mechanostimulation? In the timeframe of 6 to 9 hours after the end of the night, forces estimated to be as low as 17 mN consistently provoked electrical signaling. Similar if not larger forces would be generated by falling raindrops. The fact that mechanostimulation-induced local jasmonate signaling suggests a connection to plant defense. Under some conditions (such as penetration of developmental layer 3 by sucking invertebrates), there may be advantages of locally inducing jasmonate pathway activity. We note, however, that the long recovery periods between full-amplitude touch-response electrical signals might preclude strong stimulation of defenses. What is of interest is the connection of touch-induced jasmonate induction and phloem P-type H^+-ATPases. Insects and pathogens manipulate the activities of plasma membrane proton pumps (*45*, *46*). Our observations draw attention to the fact that organisms that can manipulate phloem AHAs may strongly affect plant defense and plant growth.

A potential link between growth rate and electrical signaling

Our findings suggest that the ability to produce mechanoresponse electrical signals relates directly or indirectly to the principal transport functions of the phloem. In nature, leaves and branches oscillate in the wind, and oscillations can activate mechanosensitive channels like MSL10 (*47*). Having a touch-response mechanism that does not fire at full power with each stimulation would allow phloem function to continue and therefore would permit normal physiological function. Related to this, when a phloem-expressed *AHA* gene in tobacco was down-regulated, the resultant plants were stunted (*48*). Here, an association between growth rate and electrical signaling was observed repeatedly in plants carrying confirmed homozygous or biallelic *aha3* mutations in *aha1* loss-of-function mutant backgrounds. While the *aha1 aha11* double mutants grew at rates similar to the WT, the growth rate/excitability association was evident in *aha3* mutants in *aha1 aha11* backgrounds (fig. S7), *aha3* mutations in the *aha11* background (where the effect was weak; fig. S8), and *aha3* mutants in the *aha1* background (Fig. 5). In summary, *AHA3* gene function in an *aha1* background is vital for mechanosensation-response electrical signaling and, in these plants, touch-induced electrical signaling is connected to overall rosette growth rate. Repeated daily bending or brushing of Arabidopsis leaves induces jasmonate production and causes thigmomorphogenesis (*10*) via transcriptional pathways which are both jasmonate dependent and independent (*14*). It remains to be seen whether the electrical activities we detected relate in any way to thigmomorphogenesis.

AHA3 protein localizes to companion cells (*34*), and proton gradients, together with K^+ transport, are essential for phloem loading (*34*, *49*). Previous reports showed that stimuli including cold-shock or current injection triggered electrical signals in the phloem and simultaneously inhibited phloem translocation in maize (*50*). Furthermore, spontaneous changes in membrane potential in trees can occur in diel time scales and are related to physiology, in particular transpiration rates, e.g., (*51*). In a fascinating parallel with our findings, a previous study (*52*) found that current injection excited leaf movements in *M. pudica*. Those leaf movements were minimal in the early morning and reached a maximum around midday. We speculate that the production of mechanostimulation-induced

electrical signals observed in our study is coupled to diel changes in phloem physiology. If so, these electrical signals (which are readily detectable at the leaf surface) could provide powerful, noninvasive read-outs of phloem status. Our results highlight the fact that, in an adult-phase plant, mechanoresponsive electrical signaling in the phloem is linked tightly to fundamental physiological processes underlying growth. Such a link is generally not the case for mechanosensation in metazoans. In animals, neuron ablation frequently annihilates specific behavioral responses without strongly affecting growth rates, e.g., (*53*).

Veins act as mechanosensors

Evidence consistent with autonomous mechanosensory properties of vascular cell populations is lacking. Using exposed primary veins attached to their WT parent plants and devoid of surrounding cells from developmental layers 1 (epidermis) and 2 (mesophyll), we found that electrical signals could be generated in response to bead impact. By contrast, the exposed primary veins of *aha1 aha3* mutants did not produce measurable electrical signals upon mechanostimulation. Moreover, and consistent with autonomous vascular mechanosensation, cytosolic Ca^{2+} transients triggered by falling beads propagated axially along exposed veins away from bead impact sites. Parallel analyses of electrical signaling in leaves and veins showed that attenuation of vascular electrical signals correlated with the reduction of signals measured on leaf surfaces. AHA3, the only individual gene product we studied which, when mutated, affects mechanostimulation-induced electrical signals, localizes to companion cells in both major and minor veins (*34*). We confirmed and extended these observations, finding AHA3 protein throughout the vasculature in primary, secondary, and tertiary veins. To conclude, the primary vasculature can act as an autonomous mechanosensory structure; our results now raise the possibility that this is the case for other vein orders.

The following aspects will need consideration in future work. Although we have calculated forces applied to leaves, these are only estimates. The time of day, plant age, growth, watering conditions, and turgor may influence the real forces experienced by plants. Albeit highly informative, the strong effects of *aha1 aha3* mutations on growth mean that WT and *aha1 aha3* plants of the same age cannot be compared. We have not measured absolute membrane potentials. This leaves open the possibility that resting membrane potentials are lower in *aha1 aha3* mutants than in the WT. Related to this, we do not know the mechanism underlying touch-response phloem membrane depolarization. Last, vein extraction inflicts substantial stress, breaking junctions between the primary and secondary vasculature (*28*). Potentially related to this, the amplitudes of depolarizations detected when exposed veins were stimulated were lower than those monitored on intact leaves. If damage to vein junctions or the stress of vein exposure is not responsible for these low amplitude depolarizations, then nonvascular cells in the vicinity of the mechanostimulated region might contribute to electrical activity measured on the leaf surface. If so, then the fascinating question of how electrical signals are coordinated between developmental layer 3 (the vasculature) and layers 1 and 2 must be addressed.

MATERIALS AND METHODS

Plant material and growth conditions

A. thaliana (Columbia, Col) plants were grown in soil in 7-cm-diameter pots in short days (10 hours light, 120 μE m^{-2} s^{-1} at 22°C and 14 hours darkness at 18°C) at 70% relative humidity. Assays were conducted with plants at the 5- to 6-week stage. Mutants in the Col background used in this study were *glr3.3* (SALK_099757) and *glr3.6* (SALK_091801) (*31*), *msl10-1* (SALK_076254) (*54*), and *aha1-7* (SALK_065288) (*18*). The *aos* mutant in the WT background was from (*24*). WT plants expressing *UBQ10promoter*::G-CaMP3 in the WT background were from (*29*).

Bead assay development

Beads were dropped from 2-cm elevations onto adaxial petiole/lamina junctions as described in Fig. 1A and fig. S1. For force calculations, serial images perpendicular to the fall path of the bead were captured with a USB 3.0 monochrome DMK 33UX174 camera (The Imaging Source, Bremen, Germany) at 1000 frames/s. These recordings were used to determine the duration of contact between the bead and the leaf. The force was calculated accordingly (fig S2).

The following borosilicate beads were used in experiments: 5 mm diameter weighing 169.7 ± 2.2 mg (n = 12) were Nr. HH56.1 from Glaskugeln Carl Roth, Germany). Estimated approximate force on lamina/petiole junction when dropped from 2-cm elevation: 76 mN; 4-mm diameter weighing 84.8 ± 1.0 mg (n = 12): Z265934-1EA, Sigma-Aldrich, USA. Estimated approximate force on lamina/petiole junction when dropped from 2-cm elevation: 38 mN; 3-mm diameter weighing 38.6 ± 1.9 mg (n = 12): Z143928-1EA, Sigma-Aldrich. Estimated approximate force on lamina/petiole junction when dropped from 2-cm elevation: 17 mN; 2-mm diameter weighing 7.1 ± 0.8 mg (n = 12): Z273627-1EA, Sigma-Aldrich. Estimated approximate force on lamina/petiole junction when dropped from 2-cm elevation: 3.2 mN.

Surface potential measurements

Silver/silver chloride electrodes were placed on the leaf 8 as described in Mousavi *et al.* (*31*). The connection between the electrode and leaf was made with a drop of 10 mM KCl in 0.5% (w/v) agar. The reference electrode was placed in the soil. Surface potential signals were recorded using LabScribe3 software (iWorx Systems Inc., Dover, NH), and signals were analyzed for depolarization amplitude and duration as described previously (*31*). The 10-mm-diameter and 10-mm-length hollow columnar plastic supports (Maxi beads 10 mm #8571, Hama, Denmark) were placed underneath and in contact with the petiole at the lamina/petiole junction (fig. S1). After a minimum 2-hour rest, beads were dropped from 2-cm height onto the adaxial lamina/petiole junction. Screening for mechanosensation-induced electrical signaling was performed in the afternoon (ZT = 6 to 9 hours) to avoid false positives.

Electrical penetration graph recordings

The electrical penetration graph (EPG) system used for recording electrical signals from phloem sieve elements was as described previously (*18*, *30*). Bead stimulation was conducted when aphids were in the E2 feeding phase according to Tjallingii (*55*). Experiments were carried out in a Faraday cage. The aphids (*B. brassicae* L.) were attached with gold wires (Ø18 μm) using water-based silver

glue (EPG Systems, Wageningen, Netherlands). Aphids were placed on leaf 8 close to the lamina/petiole junction where they generally fed on the midvein. The reference electrode was placed in the soil. A calibration pulse (50 mV) was applied before each recording. During aphid feeding, borosilicate beads 5-mm diameter weighing 169.7 ± 2.2 mg (n = 12) (Glaskugeln Nr. HH56.1, Carl Roth, Germany) were dropped onto the petiole from 2-cm height, approximately 5 mm away from the aphid electrode. No supports were placed under leaves since we found that this sometimes caused dislodgement of aphids or perturbation of the E2 phase. The maximum electrical signal amplitude was measured from the baseline. The signal duration was defined as the time from depolarization of half amplitude to repolarization of half amplitude.

Vein extraction

For monitoring electrical signals, midveins were extracted from the leaves of 6-week-old rosettes (*28*). The midveins, still attached to their parent plants, were placed on 0.7% agar containing ½ Murashige and Skoog medium and 5% (w/v) glucose for 3 to 4 hours before experiments. Note that several media were tested and that veins laid onto agar lacking glucose did not produce electrical signals. Four-millimeter borosilicate beads were used to stimulate the exposed vein from 2-cm elevations. Electrical signals were recorded at the E2 position.

Calcium imaging

Exposed midveins attached to their parent 6-week-old UBQ10::GCaMP3 plants (*29*) were placed on 0.7% agar containing ½ Murashige and Skoog medium, 5% (w/v) glucose, and 0.1% (w/v) red carmine (La Pateliere, Condom, France; used to reduce optical interference from the agar) for 4 hours before experiments. Four-millimeter borosilicate beads were used to stimulate the exposed vein from 2-cm elevations.

Microscopy

Five-week-old *Arabidopsis* plants expressing *AOSpro::NLS-3XVenus* (*27*) were bead-stimulated and maintained in the light. After 4 hours, the stimulated regions of leaves were observed with an SMZ18 stereomicroscope (Nikon Instruments Europe BV, Amsterdam, Netherlands). Images were captured with an ORCA-Flash4.0 (C11440) camera (Hamamatsu, Solothurn, Switzerland) and enhanced green fluorescent protein emission/excitation filter set (AHF analysentechnik AG, Tübingen, Germany). The same microscope, camera, and filter set were used for cytosolic Ca^{2+} imaging.

Quantitative polymerase chain reaction

Total RNA was isolated with DNA-free RNA isolation protocols (*56*). Total RNA (400 ng) was used to synthesize complementary DNA with the M-MLV Reverse Transcriptase, RNase H minus (Promega, Dübendorf, Switzerland), first-strand synthesis system. Quantitative polymerase chain reaction (PCR) analysis was performed on 10 ng of cDNA with a homemade master mix containing GoTaq polymerase (Promega) and 5× colorless GoTaq reaction buffer (Promega), 0.2 mM deoxynucleotide triphosphates, 2.5 mM $MgCl_2$, 30 nM 6-carboxy-X-rhodamine dye, and SYBR Green in a final volume of 20 µl. Ubiquitin-conjugating enzyme (*UBC21*) At5g25760 (*57*) was used as reference gene. *AOS* (At5g42650) transcripts (*58*) were displayed relative to *UBC21*.

Generation of transgenic lines

The four phloem-expressed *AHA*s chosen were *AHA1*, *AHA3*, *AHA8*, and *AHA11*. These genes were selected from supplementary dataset 1 in (*33*) by filtering for AHAs. Three guide RNAs per gene were designed in benchling website (https://benchling.com). Guide RNAs (table S1) were cloned using the oligo annealing technique (*59*) and then ligated into Gateway-entry vectors (pRU41-pRU46), which had been linearized with Bbs I (R3539S, New England BioLabs Inc. Allschwil, Switzerland) according to (*60*). Six guide RNAs (three per target gene) were assembled into the intermediate vector pSF280 using Golden Gate cloning with Bsa I (Eco31I, FD0294, Thermo Fisher Scientific. Zug, Switzerland). For simultaneously targeting of four AHAs, two intermediate vectors, each containing six guide RNAs, were cloned into destination vectors (pRU051 and pRU052) with the *PcUBI4-2::SpCas9* (*61*, *62*) and FastRed or FastGreen cassettes, respectively (*60*, *63*). WT plants were cotransformed with the two destination vectors. T1 transgenic seeds with both red and green fluorescence were planted and genotyped. Multiple CRISPR-Cas9–mutated *aha* T1 lines were selected for the absence of Cas9 in the T2 generation and genotyped to exclude potentially nonheritable somatic mutations. Two independent *aha1 aha11* double mutant lines were identified: A11 and A24. Line A11 has a 274T insertion and a deletion from 874G to 1298C in *AHA1*. Line A11 also has deletion from 275G to 287A and 6G, 687A insertion in *AHA11*. Line A24 has a 274A insertion and a deletion from 874G to 1299C in *AHA1* and insertion of 8T, deletion of 286G and 287A in *AHA11*.

Homozygous mutations in *aha3* were identified in the T1 CRISPR-Cas9–mutated generation. To maintain *aha3* mutations, the homozygous plants (male sterile) were backcrossed with WT. Fluorescent seeds indicating the presence of Cas9 were kept as a backcross population. In such a population, Cas9 could independently mutate the single WT copy of *AHA3*, which increases the frequency of homozygous *aha3* mutations. Generation of *aha1 aha3 aha11*, *aha1-7 aha3*, and *aha3 aha11* mutants: A11 line, *aha1-7* (T-DNA insertion mutant from Kumari *et al.* (*18*), and an *aha11* CRISPR-Cas9 mutant (*AHA11* coding sequence 24-689 deletion) line were transformed with *pEC1.2::zCas9i* (*64*, *65*) and appropriate guide RNAs (table S1) to target *AHA3* in respective backgrounds.

To generate a *AHA3pro::AHA3-GUS*^{PLUS} construct, the *AHA3* promoter was amplified from genomic DNA (forward primer: 5′-CGCGGGTACCCTGTCCCCACCATCCAACTTAT-3′ and reverse primer: 5′-AGCCCCCGGGCTTCTCTCTGTGCCTTCGTTCA-3′) and cloned with Kpn 1 and Xma 1 into pUC57 (L4 and R1 sites). The *AHA3* genomic coding sequence was amplified (forward primer: 5′-GGGGACAAGTTTGTACAAAAAAGCAGGCTATGGCGAGTGGCCTCGAGGAT-3′ and reverse primer: 5′-GGGGACCACTTTGTACAAGAAAGCTGGGTTAACGGTGTAGTGACCAGC-3′) and cloned into pDONR/Zeo (L1 and L2 sites) using Gateway cloning (Thermo Fisher Scientific, Zug, Switzerland). The *GUS*^{plus} gene (*66*) was cloned into pDONR (R2 and L3 sites) using Gateway cloning. These three constructs were subcloned into destination vector FR34GW (R4 and R3 sites) with a FastRed cassette (*67*) using Gateway LR cloning to generate the *AHA3pro::AHA3-GUS*^{PLUS} construct. The destination construct was transformed into the Col-0 background.

GUS staining

Soil-grown 3.5-week-old plants expressing *AHA3pro::AHA3g-GUS*^{PLUS} were fixed with 90% acetone for 30 min and washed three times with 50 mM sodium phosphate buffer (pH 7.2). Samples were vacuum-infiltrated for three times (15 min each time) with staining solution containing 10 mM EDTA, 50 mM sodium phosphate buffer (pH 7.2), 1 mM $K^4Fe(CN)^6$, 1 mM $K^3Fe(CN)^6$, 0.1% (v/v) Triton X-100, and X-Gluc (0.5 mg ml^{-1}) (*29*) and then incubated at 37°C for 16 hours. Samples were cleared with 90% ethanol and stored in 70% ethanol. Images were obtained with a VHX-6000 digital microscope (Keyence, Osaka, Japan).

Genotyping and sequencing

PCR products amplified from genomic DNA of the CRISPR-Cas9 mutant plants with primers shown in table S2A were sequenced with primers shown in table S2B. Homozygous mutations generated clear results in sequencing. To investigate heterozygous and biallelic mutations, PCR products from each plant were cloned with pGEM-T Easy Vector Systems (Promega) independently. Plasmids from single colonies were sequenced separately. In this way, two independent alleles from each single plant were identified (table S3).

Supplementary Materials

This PDF file includes:
Figs. S1 to S8
Tables S1 to S3
Legend for movie S1

Other Supplementary Material for this manuscript includes the following:
Movie S1

REFERENCES AND NOTES

1. C. Jaeger, J. Goeschl, C. Magnuson, Y. Fares, B. Strain, Short-term responses of phloem transport to mechanical perturbation. *Physiol. Plant.* **72**, 588–594 (1988).
2. S. Scherzer, W. Federle, K. Al-Rasheid, R. Hedrich, Venus flytrap trigger hairs are micronewton mechano-sensors that can detect small insect prey. *Nat. Plants* **5**, 670–675 (2019).
3. M. Krausko, Z. Perutka, M. Šebela, O. Šamajová, J. Šamaj, O. Novák, A. Pavlovič, The role of electrical and jasmonate signalling in the recognition of captured prey in the carnivorous sundew plant *Drosera capensis*. *New Phytol.* **213**, 1818–1835 (2017).
4. J. Fromm, S. Lautner, Electrical signals and their physiological significance in plants. *Plant Cell Environ.* **30**, 249–257 (2007).
5. R. Hedrich, V. Salvador-Recatalà, I. Dreyer, Electrical wiring and long-distance plant communication. *Trends Plant Sci.* **21**, 376–387 (2016).
6. T. Sibaoka, Rapid plant movements triggered by action potentials. *Bot. Mag. (Tokyo)* **104**, 73–95 (1991).
7. T. Hagihara, M. Toyota, Mechanical signaling in the sensitive plant *Mimosa pudica* L. *Plants* **9**, 587 (2020).
8. L. H. Zhou, S. B. Liu, P. F. Wang, T. J. Lu, F. Xu, G. M. Genin, B. G. Pickard, The Arabidopsis trichome is an active mechanosensory switch. *Plant Cell Environ.* **40**, 611–621 (2017).
9. M. Matsumura, M. Nomoto, T. Itaya, Y. Aratani, M. Iwamoto, T. Matsuura, Y. Hayashi, T. Mori, M. J. Skelly, Y. Y. Yamamoto, T. Kinoshita, I. C. Mori, T. Suzuki, S. Betsuyaku, S. H. Spoel, M. Toyota, Y. Tada, Mechanosensory trichome cells evoke a mechanical stimuli–Induced immune response in *Arabidopsis thaliana*. *Nat. Commun.* **13**, 1–15 (2022).
10. E. W. Chehab, C. Yao, Z. Henderson, S. Kim, J. Braam, *Arabidopsis* touch-induced morphogenesis is jasmonate mediated and protects against pests. *Curr. Biol.* **22**, 701–706 (2012).
11. D. Lee, D. H. Polisensky, J. Braam, Genome-wide identification of touch- and darkness-regulated Arabidopsis genes: A focus on calmodulin-like and *XTH* genes. *New Phytol.* **165**, 429–444 (2005).
12. R. Degli Agosti, Touch-induced action potentials in *Arabidopsis thaliana*. *Arch. des Sci.* **67**, 125–138 (2014).
13. Y. Xu, O. Berkowitz, R. Narsai, I. De Clercq, M. Hooi, V. Bulone, F. Van Breusegem, J. Whelan, Y. Wang, Mitochondrial function modulates touch signalling in *Arabidopsis thaliana*. *Plant J.* **97**, 623–645 (2019).
14. E. Darwish, R. Ghosh, A. Ontiveros-Cisneros, H. C. Tran, M. Petersson, L. De Milde, M. Broda, A. Goossens, A. Van Moerkercke, K. Khan, O. Van Aken, Touch signaling and thigmomorphogenesis are regulated by complementary CAMTA3-and JA-dependent pathways. *Sci. Adv.* **8**, eabm2091 (2022).
15. A. Van Moerkercke, O. Duncan, M. Zander, J. Šimura, M. Broda, R. Vanden Bossche, M. G. Lewsey, S. Lama, K. B. Singh, K. Ljung, J. R. Ecker, A. Goossens, A. H. Millar, O. Van Aken, A MYC2/MYC3/MYC4-dependent transcription factor network regulates water spray-responsive gene expression and jasmonate levels. *Proc. Natl. Acad. Sci. U.S.A.* **116**, 23345–23356 (2019).
16. T. Shimmen, Involvement of receptor potentials and action potentials in mechano-perception in plants. *Funct. Plant Biol.* **28**, 567–576 (2001).
17. J. Falhof, J. T. Pedersen, A. T. Fuglsang, M. Palmgren, Plasma membrane H^+-ATPase regulation in the center of plant physiology. *Mol. Plant* **9**, 323–337 (2016).
18. A. Kumari, A. Chételat, C. T. Nguyen, E. E. Farmer, Arabidopsis H^+-ATPase AHA1 controls slow wave potential duration and wound-response jasmonate pathway activation. *Proc. Natl. Acad. Sci. U.S.A.* **116**, 20226–20231 (2019).
19. M. Haruta, H. L. Burch, R. B. Nelson, G. Barrett-Wilt, K. G. Kline, S. B. Mohsin, J. C. Young, M. S. Otegui, M. R. Sussman, Molecular characterization of mutant *Arabidopsis* plants with reduced plasma membrane proton pump activity. *J. Biol. Chem.* **285**, 17918–17929 (2010).
20. R. D. Hoffmann, M. T. Portes, L. I. Olsen, D. S. C. Damineli, M. Hayashi, C. O. Nunes, J. T. Pedersen, P. T. Lima, C. Campos, J. A. Feijó, M. Palmgren, Plasma membrane H^+-ATPases sustain pollen tube growth and fertilization. *Nat. Commun.* **11**, 235 (2020).
21. W. R. Robertson, K. Clark, J. C. Young, M. R. Sussman, An *Arabidopsis thaliana* plasma membrane proton pump is essential for pollen development. *Genetics* **168**, 1677–1687 (2004).
22. M. Bear, B. Connors, M. A. Paradiso, *Neuroscience: Exploring the brain*, Jones & Bartlett Learning, LLC (2020).
23. Y. Xia, K. Yu, D. Navarre, K. Seebold, A. Kachroo, P. Kachroo, The *glabra1* mutation affects cuticle formation and plant responses to microbes. *Plant Physiol.* **154**, 833–846 (2010).
24. L. Mène-Saffrané, L. Dubugnon, A. Chételat, S. Stolz, C. Gouhier-Darimont, E. E. Farmer, Nonenzymatic oxidation of trienoic fatty acids contributes to reactive oxygen species management in *Arabidopsis*. *J. Biol. Chem.* **284**, 1702–1708 (2009).
25. C. Tretner, U. Huth, B. Hause, Mechanostimulation of *Medicago truncatula* leads to enhanced levels of jasmonic acid. *J. Exp. Bot.* **59**, 2847–2856 (2008).
26. E. M. Sehr, J. Agusti, R. Lehner, E. E. Farmer, M. Schwarz, T. Greb, Analysis of secondary growth in the Arabidopsis shoot reveals a positive role of jasmonate signalling in cambium formation. *Plant J.* **63**, 811–822 (2010).
27. P. Marhavý, A. Kurenda, S. Siddique, V. Dénervaud Tendon, F. Zhou, J. Holbein, M. S. Hasan, F. M. Grundler, E. E. Farmer, N. Geldner, Single cell damage elicits regional, nematode-restricting ethylene responses in roots. *EMBO J.* **38**, e100972 (2019).
28. E. E. Farmer, A. Kurenda, Rapid extraction of living primary veins from the leaves of *Arabidopsis thaliana*. *Protoc. Exch.* 10.1038/protex.2018.119 (2018).
29. C. T. Nguyen, A. Kurenda, S. Stolz, A. Chételat, E. E. Farmer, Identification of cell populations necessary for leaf-to-leaf electrical signaling in a wounded plant. *Proc. Natl. Acad. Sci. U.S.A.* **115**, 10178–10183 (2018).
30. V. Salvador-Recatalà, W. F. Tjallingii, E. E. Farmer, Real-time, *in vivo* intracellular recordings of caterpillar-induced depolarization waves in sieve elements using aphid electrodes. *New Phytol.* **203**, 674–684 (2014).
31. S. A. Mousavi, A. Chauvin, F. Pascaud, S. Kellenberger, E. E. Farmer, *GLUTAMATE RECEPTOR-LIKE* genes mediate leaf-to-leaf wound signalling. *Nature* **500**, 422–426 (2013).
32. J. Moe-Lange, N. M. Gappel, M. Machado, M. M. Wudick, C. S. Sies, S. N. Schott-Verdugo, M. Bonus, S. Mishra, T. Hartwig, M. Bezrutczyk, D. Basu, E. E. Farmer, H. Gohlke, A. Malkovskiy, E. S. Haswell, M. J. Lercher, D. W. Ehrhardt, W. B. Frommer, T. J. Kleist, Interdependence of a mechanosensitive anion channel and glutamate receptors in distal wound signaling. *Sci. Adv.* **7**, eabg4298 (2021).
33. Y. You, A. Sawikowska, J. E. Lee, R. M. Benstein, M. Neumann, P. Krajewski, M. Schmid, Phloem companion cell-specific transcriptomic and epigenomic analyses identify MRF1, a regulator of flowering. *Plant Cell* **31**, 325–345 (2019).
34. N. D. DeWitt, M. R. Sussman, Immunocytological localization of an epitope-tagged plasma membrane proton pump (H^+-ATPase) in phloem companion cells. *Plant Cell* **7**, 2053–2067 (1995).
35. D. Hodick, A. Sievers, The action potential of *Dionaea muscipula* Ellis. *Planta* **174**, 8–18 (1988).

36. E. Tinturier, É. Badel, N. Leblanc-Fournier, J. L. Julien, Stem bending generates electrical response in poplar. *Physiol. Plant.* **173**, 954–960 (2021).
37. I. Hug, S. Deshpande, K. S. Sprecher, T. Pfohl, U. Jenal, Second messenger–Mediated tactile response by a bacterial rotary motor. *Science* **358**, 531–534 (2017).
38. J. Kefauver, A. Ward, A. Patapoutian, Discoveries in structure and physiology of mechanically activated ion channels. *Nature* **587**, 567–576 (2020).
39. P. Hehlert, W. Zhang, M. C. Göpfert, *Drosophila* mechanosensory transduction. *Trends Neurosci.* **44**, 323–335 (2021).
40. D. Basu, E. S. Haswell, Plant mechanosensitive ion channels: An ocean of possibilities. *Curr. Opin. Plant Biol.* **40**, 43–48 (2017).
41. J. M. Codjoe, K. Miller, E. S. Haswell, Plant cell mechanobiology: Greater than the sum of its parts. *Plant Cell* **34**, 129–145 (2022).
42. C. Procko, S. Murthy, W. T. Keenan, S. A. R. Mousavi, T. Dabi, A. Coombs, E. Procko, L. Baird, A. Patapoutian, J. Chory, Stretch-activated ion channels identified in the touch-sensitive structures of carnivorous Droseraceae plants. *eLife* **10**, e64250 (2021).
43. S. Scherzer, J. Böhm, S. Huang, A. L. Iosip, I. Kreuzer, D. Becker, M. Heckmann, K. A. Al-Rasheid, I. Dreyer, R. Hedrich, A unique inventory of ion transporters poises the Venus flytrap to fast-propagating action potentials and calcium waves. *Curr. Biol.* **32**, 4255–4263.e5 (2022).
44. P. Fleurat-Lessard, S. Bouché-Pillon, C. Leloup, J.-L. Bonnemain, Distribution and activity of the plasma membrane H^+-ATPase in *Mimosa pudica* L. in relation to ionic fluxes and leaf movements. *Plant Physiol.* **113**, 747–754 (1997).
45. L. Camoni, F. Barbero, P. Aducci, M. E. Maffei, *Spodoptera littoralis* oral secretions inhibit the activity of *Phaseolus lunatus* plasma membrane H^+-ATPase. *PLOS ONE* **13**, e0202142 (2018).
46. J. M. Elmore, G. Coaker, The role of the plasma membrane H^+-ATPase in plant–Microbe interactions. *Mol. Plant* **4**, 416–427 (2011).
47. D. Tran, T. Girault, M. Guichard, S. Thomine, N. Leblanc-Fournier, B. Moulia, E. De Langre, J.-M. Allain, J.-M. Frachisse, Cellular transduction of mechanical oscillations in plants by the plasma-membrane mechanosensitive channel MSL10. *Proc. Natl. Acad. Sci. U.S.A.* **118**, e1919402118 (2021).
48. R. Zhao, V. Dielen, J.-M. Kinet, M. Boutry, Cosuppression of a plasma membrane H^+-ATPase isoform impairs sucrose translocation, stomatal opening, plant growth, and male fertility. *Plant Cell* **12**, 535–546 (2000).
49. I. Dreyer, J. L. Gomez-Porras, J. Riedelsberger, The potassium battery: A mobile energy source for transport processes in plant vascular tissues. *New Phytol.* **216**, 1049–1053 (2017).
50. J. Fromm, T. Bauer, Action potentials in maize sieve tubes change phloem translocation. *J. Exp. Bot.* **45**, 463–469 (1994).
51. Z. Hao, W. Li, X. Hao, Variations of electric potential in the xylem of tree trunks associated with water content rhythms. *J. Exp. Bot.* **72**, 1321–1335 (2021).
52. J. C. Bose, On diurnal variation of moto-excitability in mimosa. *Ann. Bot.* **27**, 759–779 (1913).
53. L. J. Elias, I. K. Succi, M. D. Schaffler, W. Foster, M. A. Gradwell, M. Bohic, A. Fushiki, A. Upadhyay, L. L. Ejoh, R. Schwark, R. Frazer, B. Bistis, J. E. Burke, V. Saltz, J. E. Boyce, A. Jhumka, R. M. Costa, V. E. Abraira, I. Abdus-Saboor, Touch neurons underlying dopaminergic pleasurable touch and sexual receptivity. *Cell* **186**, 577–590.e16 (2023).
54. E. S. Haswell, R. Peyronnet, H. Barbier-Brygoo, E. M. Meyerowitz, J.-M. Frachisse, Two MscS homologs provide mechanosensitive channel activities in the *Arabidopsis* root. *Curr. Biol.* **18**, 730–734 (2008).
55. W. F. Tjallingii, Continuous recording of stylet penetration activities by aphids. in *Aphid-plant Genotype Interactions*, R. K. Campbell, R. D. Eikenbary, Eds. (Elsevier Sci. Publ., 1990), pp. 89–99.
56. L. Oñate-Sánchez, J. Vicente-Carbajosa, DNA-free RNA isolation protocols for *Arabidopsis thaliana*, including seeds and siliques. *BMC. Res. Notes* **1**, 1–7 (2008).
57. A. Gfeller, K. Baerenfaller, J. Loscos, A. Chételat, S. Baginsky, E. E. Farmer, Jasmonate controls polypeptide patterning in undamaged tissue in wounded *Arabidopsis* leaves. *Plant Physiol.* **156**, 1797–1807 (2011).
58. A. Chini, I. Monte, A. M. Zamarreno, M. Hamberg, S. Lassueur, P. Reymond, S. Weiss, A. Stintzi, A. Schaller, A. Porzel, A. J. M. García-Mina, R. Solano, An OPR3-independent pathway uses 4, 5-didehydrojasmonate for jasmonate synthesis. *Nat. Chem. Biol.* **14**, 171–178 (2018).
59. F. Fauser, S. Schiml, H. Puchta, Both CRISPR/Cas-based nucleases and nickases can be used efficiently for genome engineering in *Arabidopsis thaliana*. *Plant J.* **79**, 348–359 (2014).
60. R. Ursache, S. Fujita, V. Dénervaud Tendon, N. Geldner, Combined fluorescent seed selection and multiplex CRISPR/Cas9 assembly for fast generation of multiple *Arabidopsis* mutants. *Plant Methods* **17**, 1–14 (2021).
61. P. Kawalleck, I. E. Somssich, M. Feldbrügge, K. Hahlbrock, B. Weisshaar, Polyubiquitin gene expression and structural properties of the *ubi4-2* gene in *Petroselinum crispum*. *Plant Mol. Biol.* **21**, 673–684 (1993).
62. J. Steinert, S. Schiml, F. Fauser, H. Puchta, Highly efficient heritable plant genome engineering using Cas9 orthologues from *Streptococcus thermophilus* and *Staphylococcus aureus*. *Plant J.* **84**, 1295–1305 (2015).
63. T. L. Shimada, T. Shimada, I. Hara-Nishimura, A rapid and non-destructive screenable marker, FAST, for identifying transformed seeds of *Arabidopsis thaliana*. *Plant J.* **61**, 519–528 (2010).
64. Z.-P. Wang, H.-L. Xing, L. Dong, H.-Y. Zhang, C.-Y. Han, X.-C. Wang, Q.-J. Chen, Egg cell-specific promoter-controlled CRISPR/Cas9 efficiently generates homozygous mutants for multiple target genes in *Arabidopsis* in a single generation. *Genome Biol.* **16**, 1–12 (2015).
65. R. Grützner, P. Martin, C. Horn, S. Mortensen, E. J. Cram, C. W. Lee-Parsons, J. Stuttmann, S. Marillonnet, High-efficiency genome editing in plants mediated by a Cas9 gene containing multiple introns. *Plant Commun.* **2**, 100135 (2021).
66. W. Broothaerts, H. J. Mitchell, B. Weir, S. Kaines, L. M. Smith, W. Yang, J. E. Mayer, C. Roa-Rodriguez, R. A. Jefferson, Gene transfer to plants by diverse species of bacteria. *Nature* **433**, 629–633 (2005).
67. K. Hématy, D. De Bellis, X. Wang, A. P. Mähönen, N. Geldner, Analysis of exocyst function in endodermis reveals its widespread contribution and specificity of action. *Plant Physiol.* **189**, 557–566 (2022).

Acknowledgments: We thank A. Kumari (National Chemical Laboratory, Pune, India) for help with cloning the *AHA3* promoter. M. Gilliham (University of Adelaide) gave valuable input concerning experimental designs. C. Hardtke and Y.-Q. Gao (both at the University of Lausanne) provided critical comments on the manuscript. **Funding:** This work was funded by the University of Lausanne and by Swiss National Science Foundation grants (31003A-175566 and 310030-205203) to E.E.F. **Author contributions:** T-H.Y. and A.C. performed genetics experiments; A.K. and T-H.Y. filmed falling beads; T-H.Y. and E.E.F. analyzed data; E.E.F. wrote the paper and agrees to serve as the author responsible for contact and ensures communication. **Competing interests:** The authors declare that they have no competing interests. **Data and materials availability:** All data needed to evaluate the conclusions in the paper are present in the paper and/or the Supplementary Materials.

Submitted 8 March 2023
Accepted 21 August 2023
Published 20 September 2023
10.1126/sciadv.adh5078